Histol Histopathol (2003) 18: 855-869
DOI: 10.14670/HH-18.855

http://www.hh.um.es

Histology and Histopathology
Cellular and Molecular Biology

Selective calcification of rat brain lesions caused by systemic administration of kainic acid

M.J. Gayoso[1], A. Al-Majdalawi[1], M. Garrosa[1], B. Calvo[2] and L. Díaz-Flores[3]

[1]Institute of Neuroscience of Castilla y León, School of Medicine, University of Valladolid, Spain,

[2]Department of Condensed Matter Physics, Crystallography and Mineralogy, University of Valladolid, Spain and

[3]Department of Anatomy, Pathology and Histology. University of La Laguna, Spain

Summary. Dystrophic calcification of previously damaged areas of nervous tissue occurs in a wide range of human diseases. The relationship between astroglial and microglial reactions and deposits of calcium salts was studied for up to five months in rats with a brain lesion produced by systemic administration of kainate. The morphology and atomic composition of the calcium salt deposits was also studied. Two types of lesions, sclerotic and liquefactive, were observed. In sclerotic lesions hyperplasia and hypertrophy of astrocytes partially substituted for the lost neurons, reaching a maximum in about twenty-five days after treatment. In liquefactive lesions, the astrocytic reaction occurred only around the liquefactive area. Microglial reaction was similar in both types of lesion and reached its highest expression in about twenty-five days. Calcium deposits were observed in the sclerotic but not in the liquefactive lesions. Clearly distinguishable granules of calcium salts were observed in sclerotic lesions under scanning electron microscopy after only five days post-injection. The size of calcified granules increased with time reaching 40 μm or more in diameter at five months. The atomic composition of these deposits, studied by X-ray microanalysis, showed a time-dependent increase in calcium concentration. While there was no clear relationship between astroglial and microglial reactions and calcium salt deposits, the systemic injection of kainate produced progressively larger and more concentrated calcium deposits in sclerotic, but not in liquefactive lesions.

Key words: Kainate, Dystrophic calcification, Astroglia, Microglia, X-ray microanalysis

Offprint requests to: Manuel J. Gayoso, Institute of Neuroscience of Castilla y León, School of Medicine, University of Valladolid, 47005 Valladollid, Spain. e-mail: gayoso@med.uva.es

Introduction

Calcifications in nervous tissue are found in a broad range of biological processes from normal ageing (Wisniewski et al., 1982) to a very wide variety of different diseases. Pathological metastatic calcification in live tissues can be caused by metabolic disorders such as hypoparathyroidism (Vakaet et al., 1985) or Fahr's disease (Ang et al., 1993). In contrast, in dystrophic calcification the minerals are deposited on areas of previously damaged nervous tissue, as happens in infections (Caldemeyer et al., 1997), tumours (Okuchi et al., 1992), after radiation and chemotherapy (Fernández-Bouzas et al., 1992), in Down's syndrome (Becker et al., 1991), dementias (Jellinger and Bancher, 1998), Parkinson's disease (Vermersch et al., 1992), Cockayne's syndrome (Ozdirim et al., 1996), epilepsy (Arnold and Kreel, 1991), cerebral hypoxia (Ansari et al., 1990; Rodriguez et al., 2001), infarction (Parisi et al., 1988), trauma (Cervós-Navarro and Lafuente, 1991), schizophrenia (Bersani et al., 1999), lupus erythematosus (Matsumoto et al., 1998) and congenital diseases (Kobari et al., 1997).

Experimentally-induced calcification in laboratory animals has been observed in spinal cord trauma (Balentine and Spector, 1977) and cerebral ischemia (Kato et al., 1995). Also, after intracerebral injection of different excitotoxins calcium deposits have been found in several areas such as substantia nigra (Nitsch and Scotti, 1992), basal ganglia (Mahy et al., 1995; Saura et al., 1995; Stewart et al., 1995), amygdaloid complex and thalamic nuclei (Saura et al., 1995). The pathogenesis of dystrophic calcification in nervous tissue is not fully understood but it is generally accepted that cellular necrosis or apoptosis may be the bases for calcium deposition (Kim, 1995). Non-atherosclerotic calcification in the brain has also been related to the glial reaction and to intracellular increase of calcium. After cerebral lesion, a local increase in the number of microglial and astroglial cells has been observed. The microglial cells increase from the first day to one week

after lesion (Acarin et al., 1999a) whereas the increase in astroglial cells occurred over a longer period, with a maximum in the first week (Acarin et al., 1999b) and remaining for several months with the consequent scar formation (Dusart et al., 1991). Astroglial and microglial reactions have been associated with the formation of calcium deposits (Saura et al., 1995; Herrmann et al., 1998).

The intracellular increase in calcium is considered one of the main events in neuronal death caused by excitotoxicity (Whetsell, 1996). This increase in calcium is caused by its entry from the extracellular compartment and also by its liberation from intracellular reservoirs leading to neuronal apoptosis and necrosis (Martin et al., 1998) through several pathogenic pathways. It has also been proposed that a high level of intracellular calcium and phosphate in apoptotic or necrotic cells is apparently the primary mechanism of calcification (Kim, 1995).

Kainate is a powerful glutamic acid agonist and has been used as an excitotoxin to produce brain lesions in studies of cerebral functions and in models of human central nervous system diseases (Bhatnagar et al., 1999; Bouilleret et al., 1999; Magnuson et al., 1999).

Intracerebral injection of kainate causes local destruction of nervous tissue (Dusart et al., 1992) whereas intracerebro-ventricular and systemic administrations are thought to affect areas with an important glutamatergic innervation (Franck and Roberts, 1990). The systemic administration of kainate to adult rats produces in the first hours a complex of motor symptoms denominated limbic seizures (Sperk et al., 1983), which has been considered as a model of human limbic seizures. The cerebral lesions observed in rats systemically treated with kainate are not uniform since in some areas they consist of neuronal loss and substitution by neuroglial cells whereas in other areas necrosis and blood vessel proliferation have been observed (Gayoso et al., 1994). In the present study we describe the calcification of brain lesions caused by intraperitoneal injection of kainic acid from two days to five months of survival time. The distribution, morphology and atomic composition of these calcium deposits as well as their relation with astroglial and microglial reactions are also described.

Materials and methods

Seven groups of 4 to 10, locally bred male adult Wistar rats were housed under standard conditions (12/12 h light/dark cycle) with free access to food and water. Care and manipulation of the animals followed the guidelines of the European Communities Council (86/609/EEC) for laboratory animal care and experimentation. Some of these animals were also used for other histological and behavioural studies. One group, which was intraperitoneally-injected with saline solution, was the control group. The remaining 6 groups of rats were intraperitoneally-injected with a single dose of 10 or 12 mg/kg of kainate. The kainate solution (0.5%) was prepared by dissolving 50 mg of kainate in 3.3 ml of NaOH and then adding 6.7 ml of 0.1M buffer phosphate pH 7.4. After a survival time of 2, 5, 10, 25, 50 or 150 days respectively the animals were anaesthetised with a mixture of 50 mg/kg of ketamine (Ketolar®Parke-Davis) and 5 mg/kg of xilacine (Rompun, Bayer AG) and transcardially perfused with buffered saline for two minutes and 4% paraformaldehyde in phosphate buffer (0.1M, pH 7.4) for 20 minutes. The brains were cryoprotected in 30% sucrose solution, frozen in dry ice and sliced in a sliding microtome at 40 μm in eight consecutive series. These series were kept frozen in 30% sucrose in phosphate buffer until staining. In each animal we studied at least one series with each of the following staining methods.

Cresyl violet (1% in bicarbonate buffer 0.1M, pH 3.6) was used as general staining. To assess the neuronal degeneration, Nadler's modification (Nadler et al., 1978) of Gallyas' method was used. Before starting the silver impregnation, the frozen sections were thawed and maintained in a 4% buffered paraformaldehyde solution for 24 h. Astroglial reaction was studied by immunohistochemical detection of glial fibrillary acidic protein (GFAP). After endogenous peroxidase blocking with 2% hydrogen peroxide in absolute methanol, free floating brain sections were incubated overnight with polyclonal anti-GFAP antibodies (Sigma G 9269), and then revealed with the standard methods using a biotinylated goat anti-rabbit IgG and a horseradish peroxidase-avidin-biotin complex (Vectastain ABC kit, Vector) with DAB as chromogen. Microglial reaction was assessed by the binding of tomato lectin (Acarin et al., 1999a) with biotinylated tomato lectin (Sigma L0651). After endogenous peroxidase blocking free floating brain sections were rinsed two times in 0.1M phosphate-buffered saline (PBS), kept ten minutes in 1% Triton X in PBS, incubated overnight in 20 μg/ml biotinylated lectin and revealed by ABC standard techniques. Histochemical staining with Alizarin red S (1% in 0.1% v/v of concentrate ammonium hydroxide, pH 6.4) was applied for calcium detection (Dahl, 1952). After Alizarin red S staining, the slides were air dried, cleared in xylene and coverslipped with Eukitt. Avoiding alcohol dehydration allows staining of lesioned areas in addition to the calcium deposits, whereas dehydration leads to a differentiation which leaves only the calcium deposits stained. After light microscopic study, selected areas of the non-stained series were mounted on carbon-coated glass slides and studied in a JEOL JM-6400 scanning electron microscope (SEM) using backscattered and secondary-electron images. The chemical composition of the selected areas was determined by energy dispersive X-ray (EDX) analysis with an electron probe micro analyzer JEOL JXA 8900 M. Student's t-test was used for data comparison and the difference was considered significant if $P < 0.05$.

Results

The general pattern of pathological changes in the affected brain regions was similar in lesioned animals

but the degree of damage was dependent on the survival time. However, there were important individual variations, since not all the injected animals showed lesioned brains. For instance, we found 5 lesioned out of 11 injected animals in the 25-day group (10 mg/kg of kainate), 7/10 in the 50-day group (10 mg/kg of kainate) and 6/11 in the 150-day group (12 mg/kg of kainate). Two types of histological lesions that we denominate sclerotic and liquefactive were found. The sclerotic type of lesions was characterized by selective focal degeneration and death of neurons in several brain regions and hyperplasia and hypertrophy of astrocytes. At the final stage studied (150 days) a glial scar was observed. This type of lesion was found mainly in olfactory bulb, anterior olfactory nucleus, Cornu Ammonis (CA) of the hippocampal formation and midline, mediodorsal and lateral thalamic nuclear groups (Fig. 1). The one denominated as a liquefactive type of lesion was characterized by non-selective neuronal death over a large area with necrosis of liquefactive type and astrocytic reaction only around the necrotic area. This lesion showed the histological characteristics of the hypoxic liquefactive necrosis. Liquefactive type of lesion prevailed in the basolateral region of the brain, in the pyriform and entorhinal cortex, and adjacent nuclei of the amydaloid complex (Fig. 1). However, adjacent to the liquefactive areas groups of neurons could be selectively affected by the sclerotic type of lesion.

Two days after kainate administration, lesions are not completely developed. The sclerotic lesions stained with cresyl violet showed shrunk neuronal bodies and nuclei, whereas in the liquefactive lesions there was rarefaction of the neuropil with a moth-eaten aspect in addition to shrunk neurons with kariolysis and kariorrhexis. The number of glial cells, easily distinguished by their smaller size, was only slightly larger than in control animals. Nadler's silver impregnation differentially stained sclerotic and liquefactive brain lesions. In the sclerotic lesions, degenerated neurons were darkly stained and fine granulated silver deposits labelled the degenerated axon terminals. The liquefactive type of lesion at this time showed a gray staining caused by very small silver granules. The degenerated neurons in these liquefactive areas were not heavily silver impregnated as they were in the sclerotic type of lesions. In the sclerotic lesions the GFAP-immunoreactive astrocytes showed numerous strongly positive processes. In the liquefactive areas the GFAP-IR was not increased. The tomato lectin binding showed an increase in the labelled microglial cells in both the sclerotic and the liquefactive type of lesions. This increase in lectin binding was caused by the increase in the individual cell binding and by a slight increase in the number of labelled cells. In addition to lesioned zones, some microglial labelled cells were also observed in the neighbouring areas. With Alizarin red S, both the sclerotic and the necrotic type of lesions showed weak staining with few and scattered stained neurons. The EDX analysis of lesioned areas did not show any detectable calcium content, their atomic composition being similar to the non-lesioned ones.

Five days after excitotoxin injection, lesions were clearly established showing outstanding histological differences with control animals (Fig. 2A,B). The number of glial cells in both sclerotic and liquefactive lesions increased. In the sclerotic lesions it was possible to differentiate some large oval glial nuclei with cresyl violet staining from others that were smaller and more elongated (Fig. 2B). The smaller, slenderer nuclei and cell bodies may correspond to migrating microglia and the others to astrocytes and other types of microglial cells. In the liquefactive lesions a larger proportion of elongated nuclei was seen. Nadler's method stained the degenerated neurons and terminals in the sclerotic lesions (Fig. 4A) more clearly (darker impregnation) than after two days. In the liquefactive lesions a diffuse brown precipitate with some stained degenerated neurons and terminals was seen with Nadler's silver impregnation (Fig. 4D). The GFAP-IR increased in the areas with sclerotic type of lesions and also around the liquefactive areas. The GFAP-IR increased not only in the lesioned areas but also in the adjacent ones. For instance, in animals with lesions located in CA1 the GFAP-IR was increased over the whole Cornu Ammonis. In contrast, the increase in glial cell number was circumscribed to the areas of neuronal destruction. Tomato lectin binding heavily stained microglial cells in lesioned areas of both sclerotic and liquefactive types. The morphology of the positive lectin cells was varied, some relatively large, round cells with short processes and others slender with longer, ramified processes. Alizarin red S stained the areas with sclerotic lesions highlighting those of the hippocampal formation (CA1

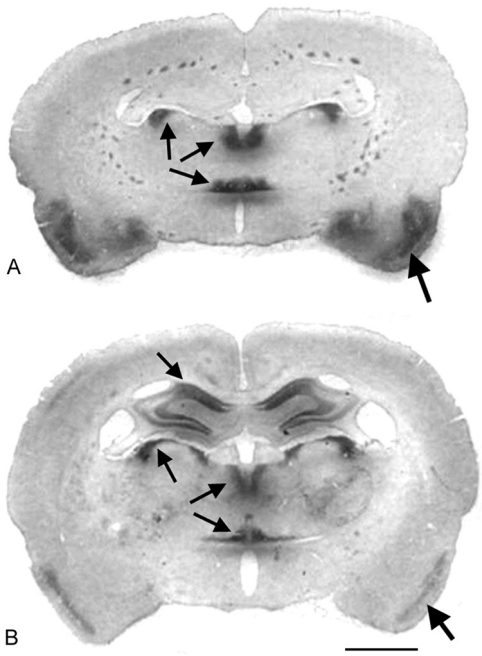

Fig. 1. Coronal brain sections of lesioned rats 10 days **(A)** and 25 days **(B)** after kainate administration. Alizarin red S stain. Large arrows: Liquefactive type of lesion in the basolateral region of the brain **(A and B)**. Small arrows: Sclerotic type of lesion in thalamus **(A)** and in thalamus and hippocampal formation **(B)**. Scale bar: 1 mm.

and CA3) and thalamus. In addition to heavily stained neuronal bodies, we observed fine red-orange granules that were more evident in the thalamic nuclei. The liquefactive areas appeared pale pink stained with Alizarin red S with some stained neuronal bodies. Under SEM it was possible to distinguish, more easily using backscattered SEM, small calcified granules of about 0.6 μm in diameter in some of the sclerotic lesions and more frequently in the thalamic nuclei (Fig. 8A). EDX analysis of these small granules showed, in addition to the O, Na, P, S, and K peaks, the calcium peaks, (Fig. 9A). The Ca/P ratio calculated in atomic percent was

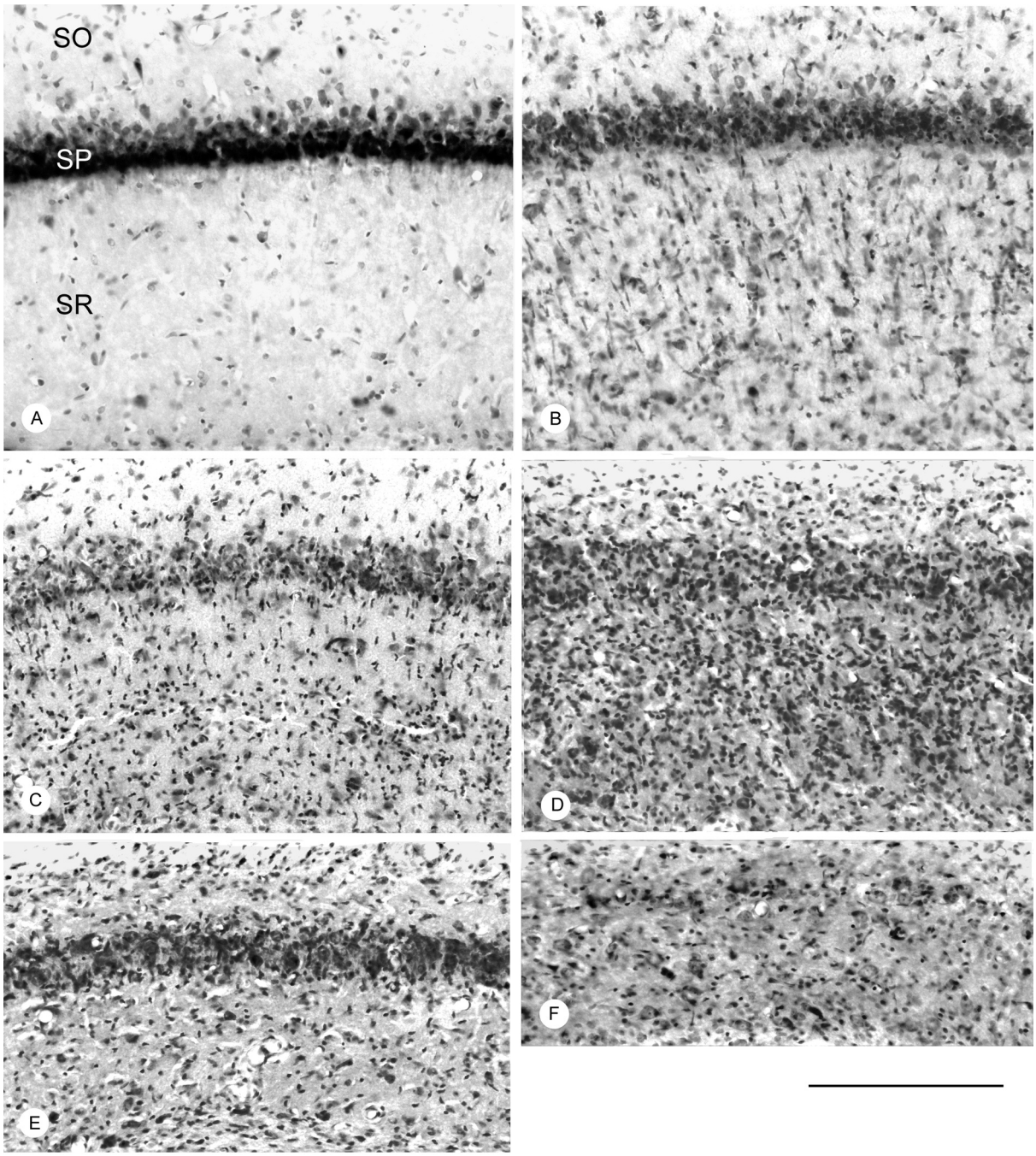

Fig. 2. Time-course of sclerotic type of brain lesion in CA1 caused by systemic injection of kainate. **A:** control. **B:** 5 days. **C:** 10 days. **D**: 25 days. **E:** 50 days. **F:** 150 days. All the photographs show only the stratum oriens (SO), stratum pyramidale (SP) and stratum radiatum (SR) of CA1. Cresyl violet stain. Scale bar: 100 μm.

0.25± 0.02 (mean ± standard error).

Ten days after kainate administration, the loss of neurons and their substitution by glial cells was easily distinguished with cresyl violet staining in both sclerotic (Fig. 2C) and liquefactive (Fig. 3A,B) lesions. The lesioned areas showed shrinkage more easily observable in highly organized areas like CA1 (Fig. 2C). The number of glial cells seemed to be increased in relation to the days before. Nadler's method clearly stained the degenerated neurons in the sclerotic-type lesion whereas in the liquefactive areas degenerated neurons were not specifically stained and the whole liquefactive area showed the characteristic brown homogeneous precipitate, with some reticular fiber-like staining of blood vessel walls. The degenerated axon terminals were more intensely labelled than days before. GFAP-IR continued to increase in the sclerotic-type lesioned areas (Fig. 5C) and also around the liquefactive ones but not in the central zone of the liquefactive necrosis (Fig. 5D). The increase in GFAP-IR was also observed in the adjacent regions. At this time, the immunoreactive astrocytes showed a more abundant cytoplasm and shorter processes except around the liquefactive areas where thick astrocytic processes constituted a sort of palisade (Fig. 5D). Lectin binding showed an increase in microglial-positive cells in both types of lesions (Fig. 6 A,C,E). In sclerotic lesions, Alizarin red S stained, in addition to some degenerated neurons, numerous small extracellular grains of about 1 μm in diameter were seen (Fig. 7A) whereas the liquefactive lesioned areas were faintly and evenly stained with some degenerated stained neurons but without any positive granules. In the sclerotic areas the SEM showed small granules of 0.64 to 1.2 μm in diameter (Fig. 8B) whereas in the liquefactive areas we did not find any granules. Backscattered electron images of these granules were clearly contrasted due to the high atomic number of calcium. EDX analysis of these granules showed a pattern similar to that of the 5-day group but with higher calcium and smaller phosphorus peaks. The Ca/P ratio was 0.44±0.05 (Fig. 10). The differences in the Ca/P ratio with the five-day group were statistically significant (P=0.037).

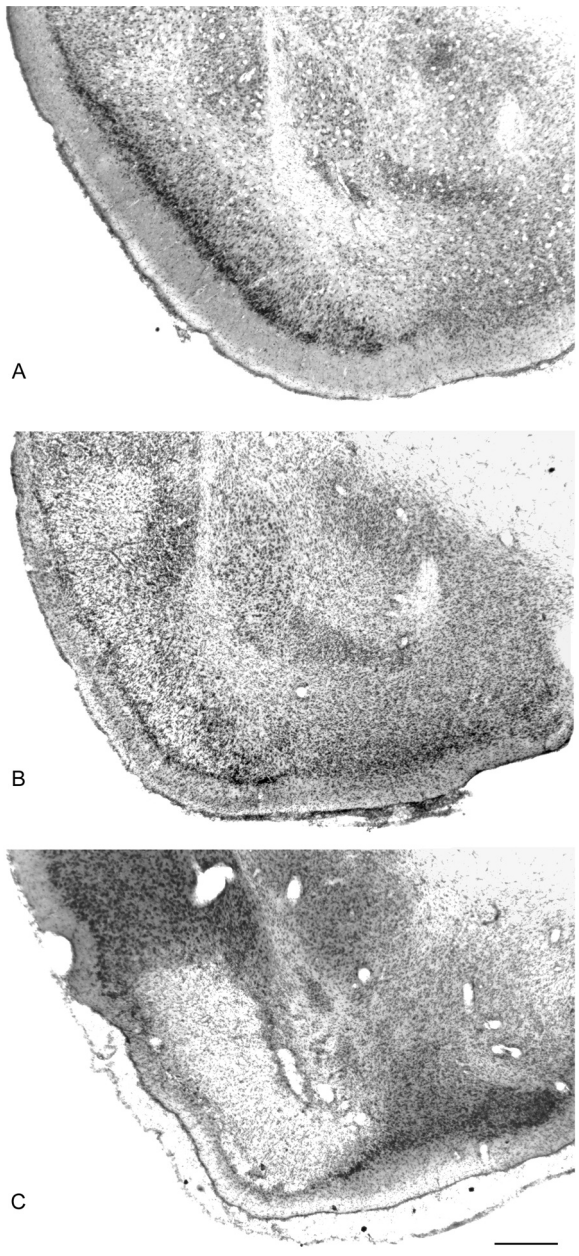

Fig. 3. Liquefactive type of lesion in the basolateral region of the brain 10 days **(B)** and 50 days **(C)** after kainate administration. **A:** control animal. Cresyl violet stain. Scale bar: 500 μm.

At 25 days the shrinking of lesioned areas was similar to that of the ten-day group but the number of glial cells seemed to increase somewhat (Fig. 2 D). With Nadler's method the impregnation of degenerated neurons and terminals was similar to the former group. The morphology of the GFAP-immunoreactive cells in the sclerotic areas was different, showing larger and positive cell bodies and less numerous, shorter processes. Around the liquefactive lesions the astrocytic palisade was more evident than before and was constituted by thicker and strongly immunoreactive processes. The binding of tomato lectin in all the lesioned areas was more intense than in preceding groups of animals. Alizarin red S showed more intense staining than before with a larger number of small stained granules only in the sclerotic areas (Fig. 7B). In these areas the SEM showed a large number of small granules of 1 μm or more in diameter (Fig. 8C). Larger granules that seemed to be made up by the growth and confluence of smaller ones were also found. X-ray microanalysis of these granules showed an increase in calcium content and a decrease in that of phosphorus (Fig. 9B) with regard to the previous group of animals. The Ca/P ratio was 1.17± 0.21 (Fig. 10) with statistically significant differences with the 10-day group (P=0.009).

The group with 50 days of survival after treatment

showed important differences regarding the 25-day group in the histological structure of lesions. After 50 days, the number of glial cells in the lesioned areas had clearly diminished (Fig. 2E). The volume of both sclerotic (Fig. 2E) and liquefactive (Fig. 3C) types of lesions decreased. In an area easy to measure, such as CA1, the thickness in coronal sections, measured from stratum oriens to stratum lacunosum-moleculare, was about 670 μm in non-lesioned animals, similar to 2 and 5 days after lesion, but after 10 and 25 days its thickness decreased to about 570 μm and it was about 470 μm after 50 days. Nadler's method heavily stained all lesioned areas with very intense labelling of neurons and terminals in the sclerotic areas (Fig. 4B) and some reticular fiber-like staining around blood vessels in the liquefactive lesions (Fig. 4C). The astrocytes in the sclerotic areas had large, irregular GFAP-IR cell bodies with less evident processes (Fig. 5E) whereas around the liquefactive lesions the astrocytic palisade appeared thicker and strongly immunoreactive (Fig. 5F). The binding of tomato lectin was usually more intense than days before in liquefactive lesions (Fig. 6B) but was less intense in sclerotic ones (Fig. 6D,F). Alizarin red S-stained granules were at this time larger and more heavily stained than those of the previous groups and were found in the sclerotic (Fig. 7C) but not in the liquefactive areas. These granules under SEM showed a high variability, from small and individual granules of about 1.5 μm to aggregates of 10 μm or more in diameter (Fig. 8D). However, the proportion of calcium and phosphorus remained similar to that in the 25-day group. The Ca/P ratio was 1.13±0.04 (Fig. 10), the difference with the preceding group not being statistically significant.

At 150 days after treatment, the number of glial cells in the sclerotic and liquefactive types of lesion was fewer than after 50 days and the volume of the lesioned areas was smaller than before (Fig. 2F). For example, CA1 now measured about 350 μm in thickness (approximately 50% of the control), the most sensitive layers being stratum oriens, stratum pyramidale and stratum radiatum (Fig. 2). In the sclerotic area Nadler's stain labelled weakly the more scarce debris of degenerated neuronal bodies and axons as well as the remaining reactive astrocytes. In the liquefactive areas Nadler's stain showed their characteristic faint, non-specific labelling and some reticular fiber-like-stain in the blood vessel walls. GFAP-IR was less positive than at day 50 post-treatment although it remained increased as compared to the control group in the sclerotic zones and around the liquefactive areas. We did not observe any special arrangement of the reactive astrocytes in

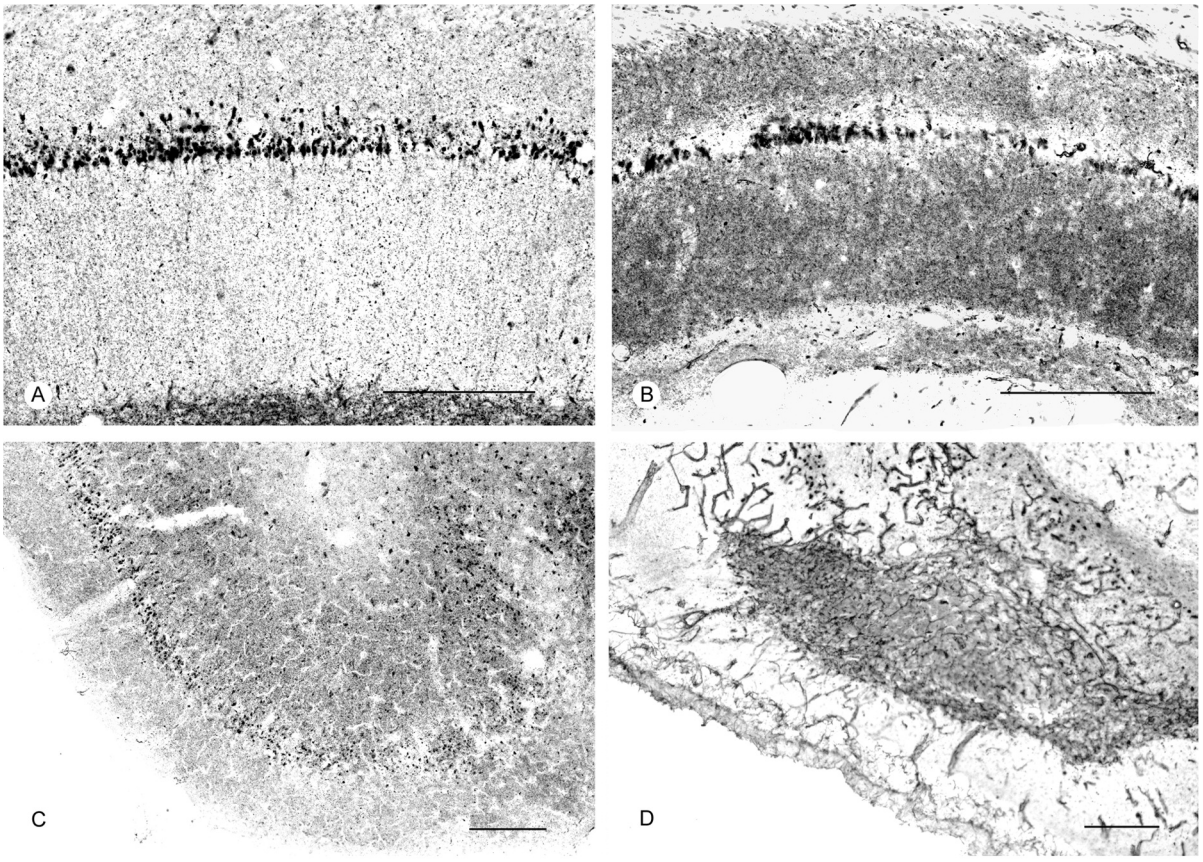

Fig. 4. Nadler's impregnation of sclerotic **(A and B)** and liquefactive **(C and D)** type of brain lesion 5 days **(A and C)** and 50 days **(B and D)** after kainate adminsitration. Scale bar: A,B, 100 μm; C,D, 200 μm.

relation to the calcification granules. The binding of tomato lectin could still be observed but to a less intense degree than at 50 days after kainate administration. Alizarin red S-positive granules were larger and more abundant (Fig. 7D) than after shorter survival times. These granules showed different sizes reaching more than 40 μm in lesioned thalamic nuclei. The SEM showed some of these granules to have an irregular shape that seemed to be formed by the confluence of smaller ones (Fig. 8E). Some of the larger granules had an oval shape and a more even surface than the smaller ones (Fig. 8F). With regard to the previous group, EDX analysis of these granules showed an increase in calcium and a decrease in phosphorus content (Fig. 9D). The Ca/P ratio was 1.33±0.14 (Fig. 10). The difference with the 50- and 25-day groups was not statistically significant. In bone prepared in a similar way to the brain sections the Ca/P ratio was 2.18±0.09, significantly

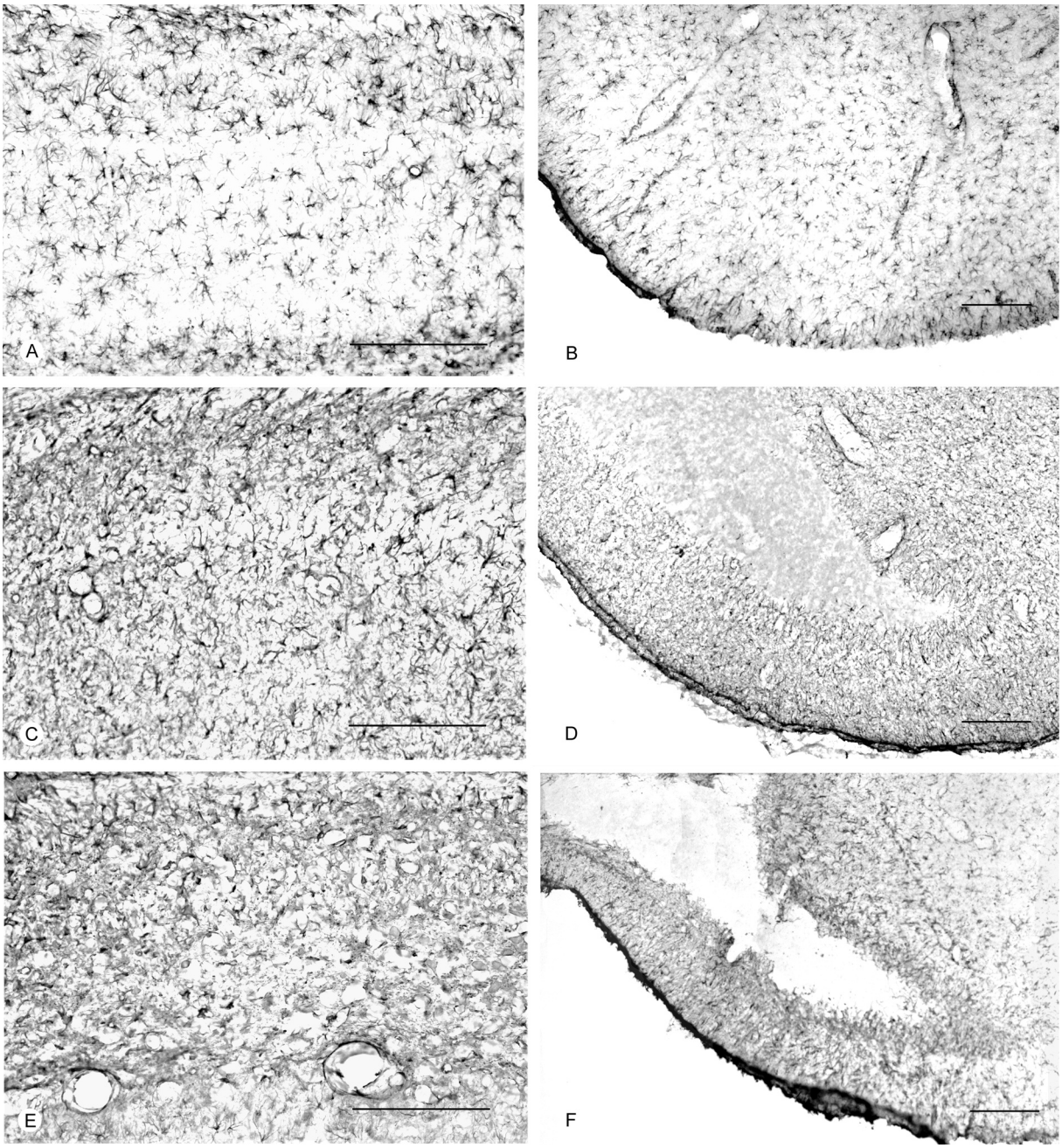

Fig. 5. GFAP-immunostaining of CA1 **(A, C and E)** and basolateral region of the brain **(B, D and F)** of control **(A and B)** and after 10 days **(C and D)** and 50 days **(E and F)** of kainate administration. Scale bar : 100 μm (A, C and E) and 200 μm (B, D and F).

higher than in all the calcified lesions observed.

Discussion

The pattern of brain lesions observed in our experiments is similar to that previously described after systemic administration of kainate (Schwob et al., 1980; Sperk, et al., 1983, 1985; Sperk, 1994) but we consider that the two types of lesions that we denominate sclerotic and liquefactive lesions may be produced by different pathogenic mechanisms and have different evolution in relation to the deposit of calcium salts. Our two lesion types refer to the type of histological change and do not correspond to mechanisms of cell death such as necrosis, apoptosis or any intermediate form between them (Martin et al., 1998).

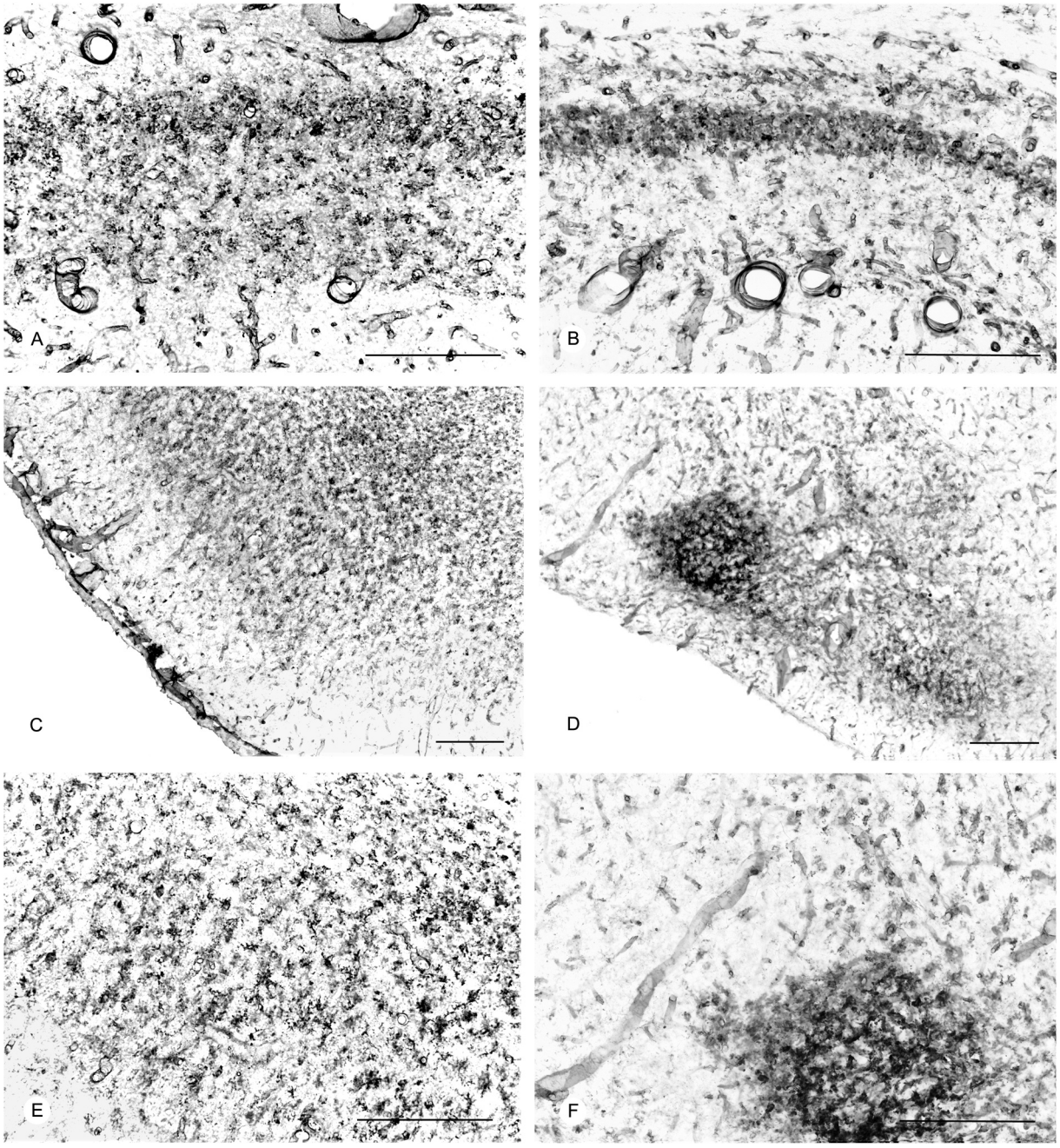

Fig. 6. Tomato lectin binding in CA1 **(A and B)** and basolateral region of the brain **(C, D, E and F)** 10 days **(A, C and E)** and 50 days **(B, D and F)** after kainate administration. E and F are details of the C and D figures respectively. Scale bar = 100 μm.

The sclerotic type of lesion may be caused by kainate acting as a neurotransmitter by directly or indirectly promoting the selective death of specific groups of neurons followed by the proliferation of astrocytes and microglial cells. In contrast, the second type of lesion is similar to that classically described as liquefactive necrosis and also to that described by DeGirolami et al. (1984) as total necrosis, with destruction of both gray and white matter, an inner zone of liquefaction and sharp margins containing astrocytes and mononuclear cells. This type of lesion could be caused by kainate administration which would produce a generalized brain edema (Sperk et al., 1983) originating compression and hypoxia in the basal region of the brain. The massive swelling of astrocytes (Lassmann et al., 1984) and cytotoxic brain edema (Seitelberger et al., 1990) observed after systemic injection of kainate can also contribute to this lesion.

The cellular mechanism through which kainate produces neuronal destruction is not well understood yet. The excitotoxic action of kainate is performed, in the first place, on neurons bearing mainly kainate receptors. Kainate, in a large enough dosage, may cause an apoptotic type of neuronal death upon this type of neuron similar but not identical to the physiological apoptosis observed during central nervous system development (Martin, et al., 1998). In contrast, the hyperstimulation of N-methyl-D-aspartate (NMDA) receptors would cause a necrosis type of neuronal death in neurons with predominance of this type of receptor. In our experiments, the neuronal death caused by the systemic injection of kainate is histologically more similar to necrosis than to apoptosis, which is in agreement with previous studies in which the intraperitoneal injection of kainate in adult rats produced neuronal death with morphology mainly similar to necrosis and with a small number of apoptotic-like cells (Ferrer et al., 1997). However, it has been described that some of these neurons with morphological signs of necrosis are stained with the terminal deoxynucleotidyl transferase dUTP nick-end labeling (TUNEL) technique and yield biochemical evidence of ladder fragmentation of DNA (Fujikawa et al., 2000). These data, contradictory in appearance, would support the hypothesis that the neuronal death caused by excitotoxins may take place in a continuum between apoptosis and necrosis similar to apoptosis when the excitotoxin acts on non-NMDA receptors and more

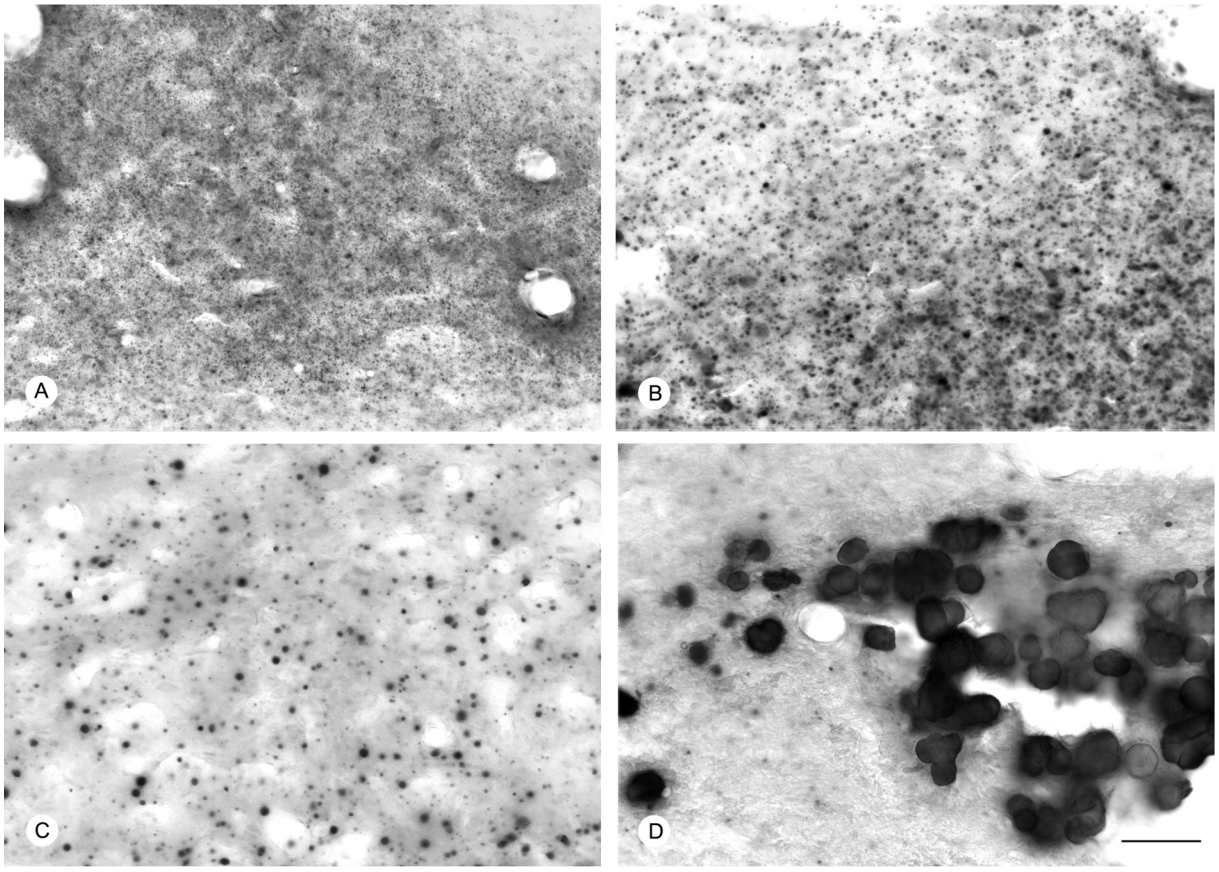

Fig. 7. Alizarin red S staining of the basal thalamus around the reuniens nucleus at 10 **(A)**, 25 **(B),** 50 **(C)** and 150 days **(D)** after kainate administration. Note the increasing size of calcium salt deposits. Scale bar : 50 μm.

similar to necrosis after stimulation of NMDA receptors (Portera-Cailliau et al., 1997; Martin, et al., 1998). Our results indicate that systemic injection of kainate is the cause of selective loss of neurons predominantly bearing NMDA receptors. For instance, in the hippocampal formation we observed neuronal death predominantly of necrosis type in CA1 whose neurons have receptors of NMDA type, whereas in CA3 and CA4, where kainate receptors are the most abundant (Cotman et al., 1987), the lesioned neurons were less numerous. A possible explanation of these results could be that kainate, acting on its specific receptors on CA3 and CA4 pyramidal neurons, causes the death of these neurons or, since these neurons are glutamatergic, the axonal release of glutamate. Glutamate would then act upon CA1 pyramidal neurons indirectly causing the cellular death with a morphology similar to necrosis. A similar mechanism has been proposed to interpret the epileptic

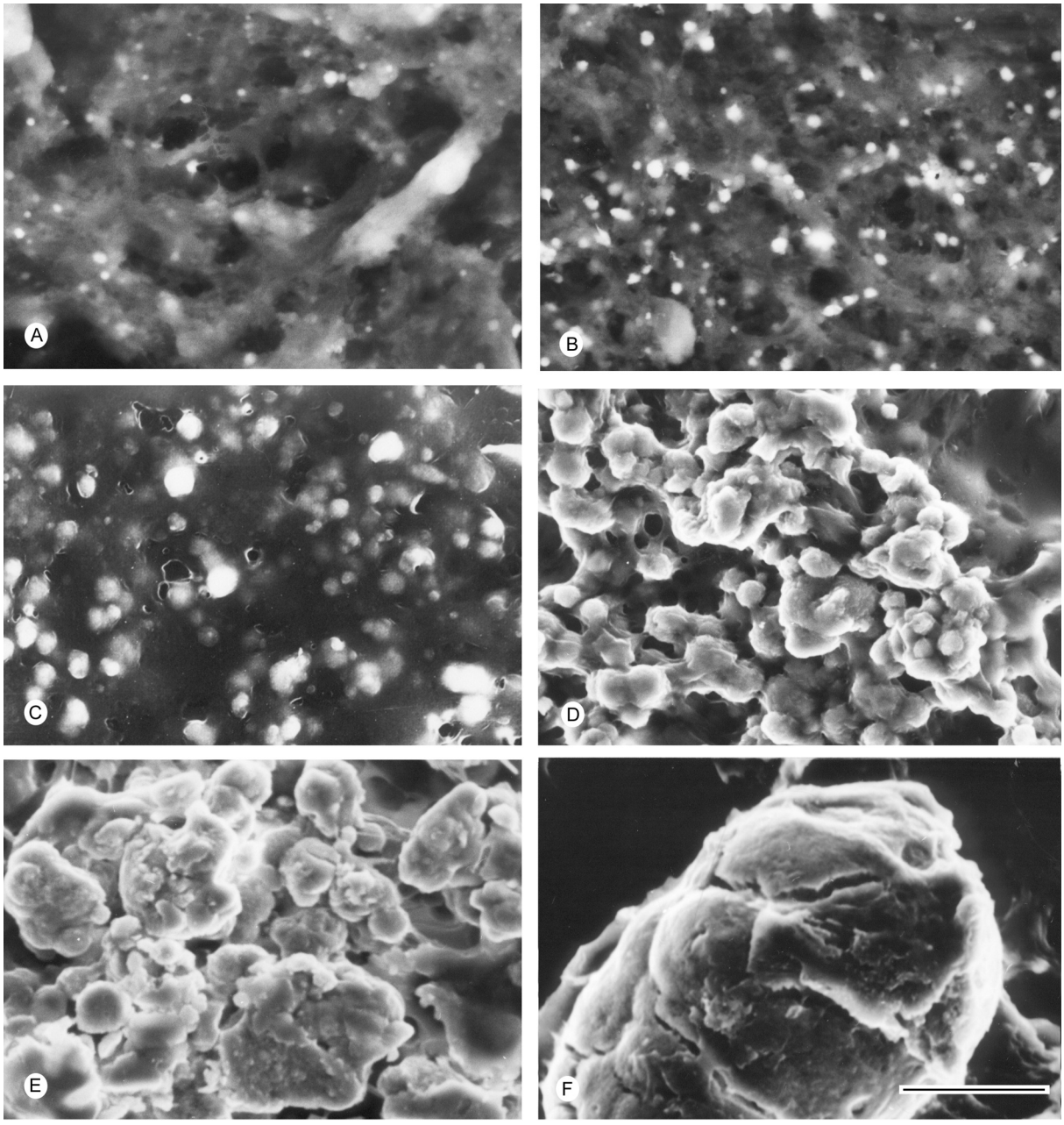

Fig. 8. Backscattered scanning electron micrographs of the deposits of calcium salts in the sclerotic type of lesions 5 **(A)**, 10 **(B)**, 25 **(C)**, 50 **(D)** and 150 days **(E and F)** after kainate administration. At the final stage large aggregates and also very large rounded granules are observed. Scale bar: 10 μm.

crisis and the subsequent lesions produced by systemic administration of kainate (Fujikawa et al., 2000) and also to explain the discrepancy between neuronal death caused by excitotoxins and the distribution of glutamatergic receptor in the amygdaloid complex (Tuunanen et al., 1999). In this study the authors observed that the distribution of neuronal damage in the amygdaloid nuclei differs from the distribution of kainate receptors.

The neuronal death caused by ischemia seems to be of the necrotic type (Martin et al., 1998) although morphological and biochemical characteristics of necrosis as well as of apoptosis have been described in ischemic neuronal death, with variations depending on severity and instauration rate of the ischemia (Benchoua et al., 2001).

The increasing of GFAP-IR that we observed in the first days post-lesion could be due to alterations in

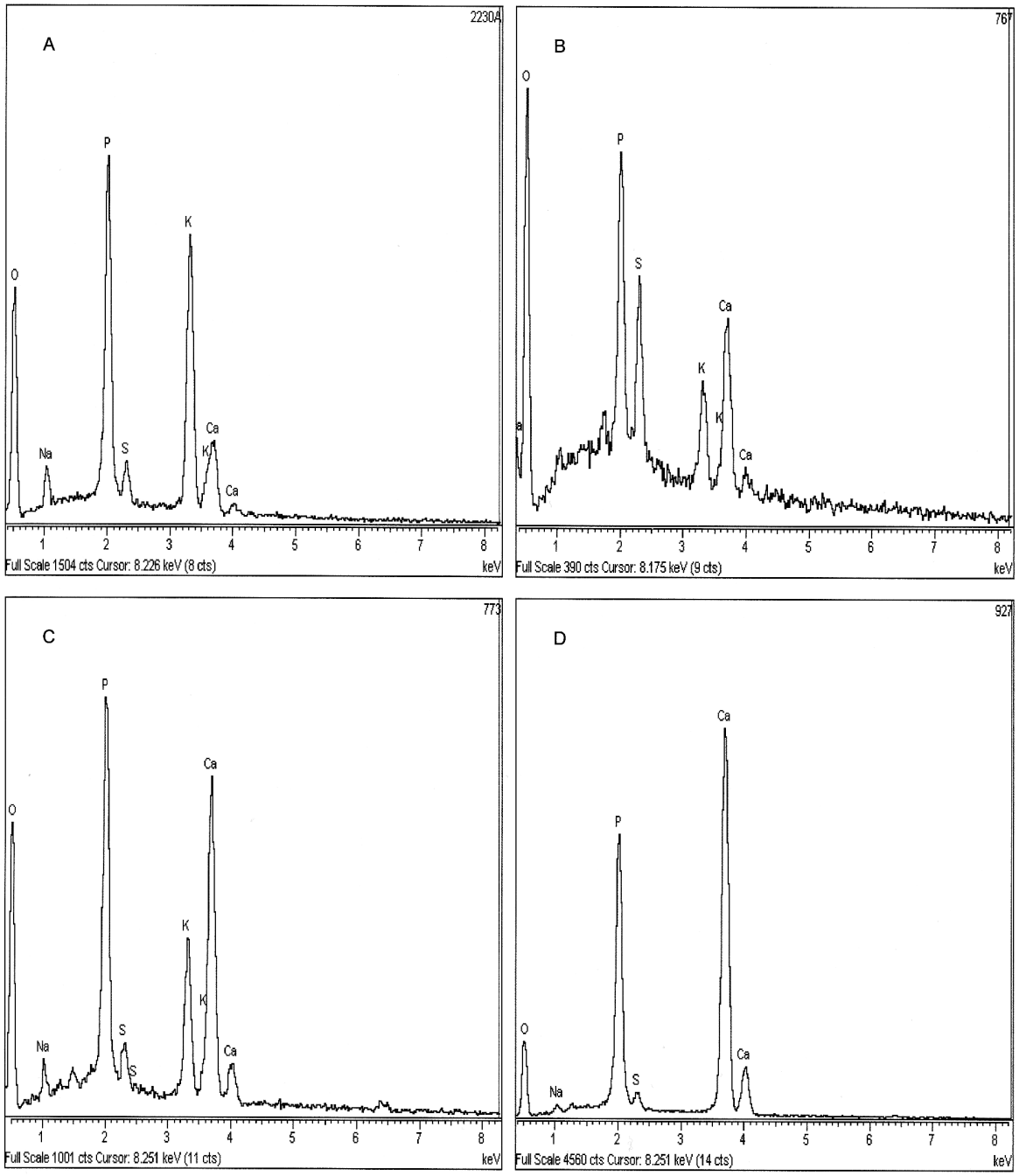

Fig. 9. Chemical composition of salt deposits determined by energy dispersive X-ray analysis 5 **(A)**, 25 **(B)**, 50 **(C)** and 150 days **(D)** after kainate administration. Note the increase in calcium concentration.

cytoskeleton proteins produced by the post-injury swelling and the exposition of antigenic sites after depolymerization of GFAP filaments (Dusart et al., 1991).

In a study with a similar administration of kainate, Gramsbergen and van den Berg (1994) found an increase of GFAP in all the studied areas. This GFAP increase reached the highest value about 28 days after treatment, remaining high up to 6 months, the longest period studied. Our results are in agreement with these observations since we observed the highest GFAP-IR on day 25, and it remained high up to 150 days. However, we found some discrepancies with the results of Gramsbergen and van den Berg (1994) since they found the highest GFAP increase in pyriform cortex and amygdaloid complex where we found liquefactive necrosis with only a surrounding area of hypertrophic astrocytes.

In our experiments the microglial reaction was similar in both sclerotic and liquefactive types of lesions. An increase in microglial-like reactive cells was seen in the lesioned areas from 2 days onwards reaching a maximum in lectin binding between 25 and 50 days and remaining visible at 5 months. In the first days after lesion we were not able to determine if the increased number of lectin-positive cells was produced by migration from neighbouring areas, by cellular division of resident microglial cells or by both mechanisms. The activation of microglial cells by kainate or hypoxia seems to be a very fast phenomenon that can be observed in vitro after twenty minutes (Abraham et al., 2001). In brain lesions without blood vessel breaking such as intraventricular injection of kainate, one of the earlier events is the enlarged microglial cell processes (Streit et al., 1999) and migration of microglial cells from surrounding areas (Akiyama et al., 1994). Also, proliferation of resident microglia has been shown after intracerebral injection of kainate (Marty et al., 1991) and at the periphery of human cerebral infarction up to day 3 post-infarction (Postler et al., 1997). Probably, both mechanisms are involved in this microglial reaction in the first days after lesion with subsequent participation of leukocytes migrating from blood vessels (Marty, 1991; Akiyama et al., 1994). After intracerebral injection, the microglial reaction shows a clear diminution at 30 days, therefore decreasing faster than in our experiments (Marty et al., 1991; Streit et al., 1999). Also, after deafferentation of vestibular and cochlear nuclei the microglial reaction reached a maximum at 8-14 day and lasted for 42 days (Campos Torres et al., 1999). We found a decrease in lectin labelling after 50 days lasting to the end of our observations. These differences could be due in part to the different methods used to stain the microglial cells, and also because the lesions caused by systemic kainate could recruit less phagocytic cells from blood vessels; thus microglial cells will remain for a larger time to remove the cellular debris.

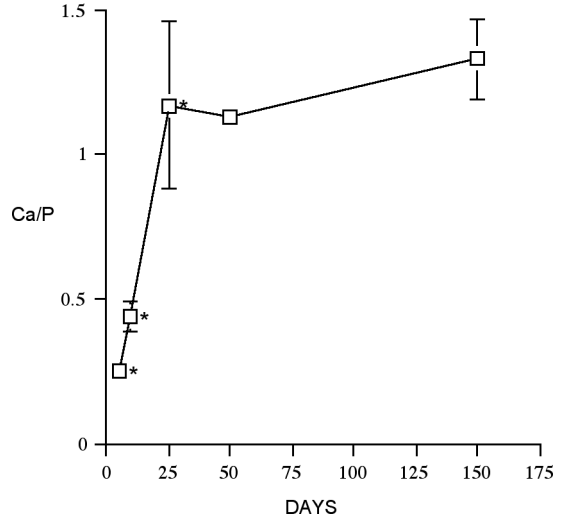

Fig. 10. Time-course of the calcium/phosphorus proportion in the deposits of calcium salts in the sclerotic lesion caused by kainate administration. Mean ± SE (*P<0.05).

The Alizarin red S staining without alcohol differentiation reveals not only the calcium salt deposits but also the sclerotic type of lesioned areas without calcification. This method could stain areas with specific ionic composition, possibly accumulation of calcium ions, since the pictures obteined with Alizarin red S are very similar to the ^{45}Ca autoradiograms obtained after systemic kainate injection (Gramsbergen and van den Berg, 1994).

It is possible that in the sclerotic type of lesion calcium concentration was increased but we found deposits of calcium salts only in some of these areas. Selective calcification has been described after intracerebral injection of excitotoxin because some areas such as substantia nigra and globus pallidus developed calcification whereas the striatum and septum did not (Nitsch and Schaefer, 1990; Nitsch and Scotti, 1992; Mahy et al., 1995). We did not find Alizarin red S staining or calcium salt deposits in the liquefactive type of lesions perhaps because in these areas cellular death is produced too suddenly. Also, after intracerebral injections of excitotoxin the calcification does not occur in the injection site but in areas some distance apart (Nitsch and Schaefer, 1990).

The injection of excitotoxins causes an increase in the intracellular calcium (Nitsch and Scotti, 1992; Bernal et al., 2000) which may be responsible for most destructive processes in the cells (Trump et al., 1992; Kim, 1995). Also in cellular apoptosis the decrease in ATP synthesis increases intracellular phosphate and these increases of calcium and phosphate may produce intracellular deposits of calcium phosphate. These mechanisms could explain the calcification of neurons such as proposed by Mahy et al. (1995). In our experiments we observed some scattered Alizarin red S-stained neurons in the lesioned areas but the deposits of

calcium salts seemed to start as small granules in the extracellular matrix. The relationships between lesioned neurons and altered extracellular matrix are not well known. In this context it has been proposed that dying neurons may discharge the intracellular calcium and phosphate to the extracellular space by membranous vesicles or cytoplasmic blebs (Kim, 1995). In the formation of this altered extracellular matrix astrocytes may also play a significant role (Herrmann et al., 1998; Nitsch and Scotti, 1992). The membranous degradation products resulting from cellular destruction could serve to nucleate calcium phosphate deposits (Kim, 1995).

Our observations do not indicate any differential relationship between astroglia or microglia reaction and calcification. Astrocytes proliferate in all the sclerotic lesions but calcification was observed only in some of them. Nevertheless, we do not discard the idea that the astrocytes could play an important role in the formation of organic matrix on which the calcium salts were deposited (Herrmann et al., 1998). Microglia has also been considered as a factor in dystrophic brain calcification since after intracerebral injection of ibotenate in the globus pallidus astroglial and microglial reaction occurs with calcification. However, when the septum is injected an astroglial reaction takes place but there is no microglial reaction or calcification (Saura et al., 1995). The importance of the role played by microglia in dystrophic calcification is supported by the observation (Petegnief et al., 1999) that the microglial reaction and calcification induced by intracerebral injection of AMPA are inhibited by an AMPA antagonist which does not inhibit the astroglial reaction.

In our experiments we found a microglial reaction in both sclerotic and liquefactive types of lesions and only calcification in some of the sclerotic areas. Therefore, our observations indicate that calcification occurs in areas with chronic astroglial and microglial reactions but that these reactive processes are not sufficient to produce deposits of calcium salts.

The general development of calcium deposits in our study is quite similar to that previously described (Kato et al., 1995). These authors found fine Alizarin red S-positive granules containing calcium in gerbil brain after short periods of cerebral ischemia and one month of survival, and at six months large calcium concretions. In our observations very small granules containing calcium and phosphate were observed earlier, at 5 days post-treatment. Two months after intracerebral injection of kainate small deposits of about 4 μm in diameter and larger ones about 16 μm in diameter were found (Bernal et al., 2000). Our results are comparable to the latter because we found granules of 1.5-10 μm or more in diameter at 50 days. We consider, as proposed by Nitsch and Scotti (1992) that the size of the calcium phosphate is time dependent.

Our X-ray microanalysis yielded a chemical composition of calcium and phosphorus similar to that obtained after intracerebral injection of excitotoxins (Herrmann et al., 1998; Mahy et al., 1999) and compatible with calcium phosphate in the form of hydroxyapatite (Mahy et al., 1999). We have observed a gradual increase in Ca/P proportion, but it never reached values comparable with those observed in bone. Lower Ca/P ratio seems to correspond with a less organized, porous apatitic small crystals as described in other pathological calcifications (Poggy et al., 2001). Nevertheless, information concerning the mineral composition of dystrophic calcification is too limited to allow us to establish firm conclusions on this topic.

In conclusion, the systemic injection of kainate produces calcium phosphate deposits in sclerotic but not in liquefactive type of lesions with a progressive increase in size and in calcium concentration.

Acknowledgements. We thank Luis Santiago and Teresa Rodríguez for technical assistance. This work was supported by FIS Grants 95/1558 and 01/0772.

References

Abraham H., Losonczy A., Czeh G. and Lazar G. (2001). Rapid activation of microglial cells by hypoxia, kainic acid, and potassium ions in slice preparations of the rat hippocampus. Brain Res. 906, 115-126.

Acarin L., Gonzalez B., Castro A.J. and Castellano B. (1999a). Primary cortical glial reaction versus secondary thalamic glial response in the excitotoxically injured young brain: microglial/macrophage response and major histocompatibility complex class I and II expression. Neuroscience 89, 549-565.

Acarin L., Gonzalez B., Hidalgo J., Castro A.J. and Castellano B. (1999b). Primary cortical glial reaction versus secondary thalamic glial response in the excitotoxically injured young brain: astroglial response and metallothionein expression. Neuroscience 92, 827-839.

Akiyama H., Tooyama I., Kondo H., Ikeda K., Kimura H., McGeer E.G. and McGeer P.L. (1994). Early response of brain resident microglia to kainic acid-induced hippocampal lesions. Brain Res. 635, 257-268.

Ang L.C., Rozdilsky B., Alport E.C. and Tchang S. (1993). Fahr's disease associated with astrocytic proliferation and astrocytoma. Surg. Neurol. 39, 365-369.

Ansari M.Q., Chincanchan C.A. and Armstrong D.L. (1990). Brain calcification in hypoxic-ischemic lesions: an autopsy review. Pediatr. Neurol. 6, 94-101.

Arnold M.M. and Kreel L. (1991). Asymptomatic cerebral calcification--a previously unrecognized feature. Postgrad. Med. J. 67, 147-153.

Balentine J.D. and Spector M. (1977). Calcification of axons in experimental spinal cord trauma. Ann. Neurol. 2, 520-523.

Becker L., Mito T., Takashima S. and Onodera K. (1991). Growth and development of the brain in Down syndrome. Prog. Clinic. Biol. Res. 373, 133-152.

Benchoua A., Guegan C., Couriaud C., Hosseini H., Sampaio N., Morin D. and Onteniente B. (2001). Specific caspase pathways are activated in the two stages of cerebral infarction. J. Neurosci. 21, 7127-7134.

Bernal F., Saura J., Ojuel J. and Mahy N. (2000). Differential vulnerability of hippocampus, basal ganglia, and prefrontal cortex to

long-term NMDA excitotoxicity. Exp. Neurol. 161, 686-695.

Bersani G., Garavini A., Taddei I., Tanfani G. and Pancheri P. (1999). Choroid plexus calcification as a possible clue of serotonin implication in schizophrenia. Neurosci. Lett. 259, 169-172.

Bhatnagar T., Chitravanshi V.C. and Sapru H.N. (1999). Cardiovascular responses to microinjections of excitatory amino acids into the area postrema of the rat. Brain Res. 822, 192-199.

Bouilleret V., Ridoux V., Depaulis A., Marescaux C., Nehlig A. and Le Gal La Salle G. (1999). Recurrent seizures and hippocampal sclerosis following intrahippocampal kainate injection in adult mice: electroencephalography, histopathology and synaptic reorganization similar to mesial temporal lobe epilepsy. Neuroscience 89, 717-729.

Caldemeyer K.S., Mathews V.P., Edwards-Brown M.K. and Smith R.R. (1997). Central nervous system cryptococcosis: parenchymal calcification and large gelatinous pseudocysts. Am. J. Neuroradiol. 18, 107-109.

Campos Torres A., Vidal P.P. and de Waele C. (1999). Evidence for a microglial reaction within the vestibular and cochlear nuclei following inner ear lesion in the rat. Neuroscience 92, 1475-1490.

Cervós-Navarro J. and Lafuente J.V. (1991). Traumatic brain injuries: structural changes. J. Neurol. Sci. 103 Suppl, S3-14.

Cotman C.W., Monaghan D.T., Ottersen O.P. and Storm-Mathisen J. (1987). Anatomical organization of excitatory amino acid receptors and their pathways. Trends Neurosci. 10, 273-280.

Dahl L.K. (1952). A simple and sensitive histochemical method for calcium. Proc. Soc. Exp. Biol. Med. 80, 474-479.

DeGirolami U., Crowell R.M. and Marcoux F.W. (1984). Selective necrosis and total necrosis in focal cerebral ischemia. Neuropathologic observations on experimental middle cerebral artery occlusion in the macaque monkey. J. Neuropathol. Exp. Neurol. 43, 57-71.

Dusart I., Marty S. and Peschanski M. (1991). Glial changes following an excitotoxic lesion in the CNS--II. Astrocytes. Neuroscience 45, 541-549.

Dusart I., Marty S. and Peschanski M. (1992). Demyelination, and remyelination by Schwann cells and oligodendrocytes after kainate-induced neuronal depletion in the central nervous system. Neuroscience 51, 137-148.

Fernández-Bouzas A., Ramirez Jiménez H., Vázquez Zamudio J., Alonso-Vanegas M. and Mendizabal Guerra R. (1992). Brain calcifications and dementia in children treated with radiotherapy and intrathecal methotrexate. J. Neurosurg. Sci. 36, 211-214.

Ferrer I., Planas A.M. and Pozas E. (1997). Radiation-induced apoptosis in developing rats and kainic acid-induced excitotoxicity in adult rats are associated with distinctive morphological and biochemical c-Jun/AP-1 (N) expression. Neuroscience 80, 449-458.

Franck J.E. and Roberts D.L. (1990). Combined kainate and ischemia produces 'mesial temporal sclerosis'. Neurosci. Lett. 118, 159-163.

Fujikawa D.G., Shinmei S.S. and Cai B. (2000). Kainic acid-induced seizures produce necrotic, not apoptotic, neurons with internucleosomal DNA cleavage: implications for programmed cell death mechanisms. Neuroscience 98, 41-53.

Gayoso M.J., Primo C., Al-Majdalawi A., Fernández J.M., Garrosa M. and Iñiguez C. (1994). Brain lesions and water-maze learning deficits after systemic administration of kainic acid to adult rats. Brain Res. 653, 92-100.

Gramsbergen J.B. and van den Berg K.J. (1994). Regional and temporal profiles of calcium accumulation and glial fibrillary acidic protein levels in rat brain after systemic injection of kainic acid. Brain Res. 667, 216-228.

Herrmann G., Stunitz H. and Nitsch C. (1998). Composition of ibotenic acid-induced calcifications in rat substantia nigra. Brain Res. 786, 205-214.

Jellinger K.A. and Bancher C. (1998). Senile dementia with tangles (tangle predominant form of senile dementia). Brain Pathol. 8, 367-376.

Kato H., Araki T., Itoyama Y. and Kogure K. (1995). Calcium deposits in the thalamus following repeated cerebral ischemia and long-term survival in the gerbil. Brain Res. Bull. 38, 25-30.

Kim K.M. (1995). Apoptosis and calcification. Scann. Microsc. 9, 1137-75; discussion 1175-1178.

Kobari M., Nogawa S., Sugimoto Y. and Fukuuchi Y. (1997). Familial idiopathic brain calcification with autosomal dominant inheritance. Neurology 48, 645-649.

Lassmann H., Petsche U., Kitz K., Baran H., Sperk G., Seitelberger F. and Hornykiewicz O. (1984). The role of brain edema in epileptic brain damage induced by systemic kainic acid injection. Neuroscience 13, 691-704.

Magnuson D.S., Trinder T.C., Zhang Y.P., Burke D., Morassutti D.J. and Shields C.B. (1999). Comparing deficits following excitotoxic and contusion injuries in the thoracic and lumbar spinal cord of the adult rat. Exp. Neurol. 156, 191-204.

Mahy N., Bendahan G., Boatell M. L., Bjelke B., Tinner B., Olson L. and Fuxe K. (1995). Differential brain area vulnerability to long-term subcortical excitotoxic lesions. Neuroscience 65, 15-25.

Mahy N., Prats A., Riveros A., Andres N. and Bernal F. (1999). Basal ganglia calcification induced by excitotoxicity: an experimental model characterised by electron microscopy and X-ray microanalysis. Acta Neuropathol. (Berl) 98, 217-225.

Martin L.J., Al-Abdulla N.A., Brambrink A.M., Kirsch J.R., Sieber F.E. and Portera-Cailliau C. (1998). Neurodegeneration in excitotoxicity, global cerebral ischemia, and target deprivation: A perspective on the contributions of apoptosis and necrosis. Brain Res. Bull. 46, 281-309.

Marty S., Dusart I. and Peschanski M. (1991). Glial changes following an excitotoxic lesion in the CNS--I. Microglia/macrophages. Neuroscience 45, 529-539.

Matsumoto R., Shintaku M., Suzuki S. and Kato T. (1998). Cerebral perivenous calcification in neuropsychiatric lupus erythematosus: a case report. Neuroradiology 40, 583-586.

Nadler J.V., Perry B.W. and Cotman C.W. (1978). Intraventricular kainic acid preferentially destroys hippocampal pyramidal cells. Nature 271, 676-677.

Nitsch C. and Schaefer F. (1990). Calcium deposits develop in rat substantia nigra but not striatum several weeks after local ibotenic acid injection. Brain Res. Bull. 25, 769-773.

Nitsch C. and Scotti A.L. (1992). Ibotenic acid-induced calcium deposits in rat substantia nigra. Ultrastructure of their time-dependent formation. Acta Neuropathol. 85, 55-70.

Okuchi K., Hiramatsu K., Morimoto T., Tsunoda S., Sakaki T. and Iwasaki S. (1992). Astrocytoma with widespread calcification along axonal fibres. Neuroradiology 34, 328-330.

Ozdirim E., Topçu M., Ozön A. and Cila A. (1996). Cockayne syndrome: review of 25 cases. Pediatr. Neurol. 15, 312-316.

Parisi J., Place C. and Nag S. (1988). Calcification in a recent cerebral infarct--radiologic and pathologic correlation. Can. J. Neurol. Sci. 15, 152-155.

Petegnief V., Saura J., Dewar D., Cummins D.J., Dragunow M. and

Mahy N. (1999). Long-term effects of alpha-amino-3-hydroxy-5-methyl-4-isoxazole propionate and 6-nitro-7-sulphamoylbenzo(f)quinoxaline-2,3-dione in the rat basal ganglia: calcification, changes in glutamate receptors and glial reactions. Neuroscience 94, 105-115.

Poggy S.H., Bostrom K.I., Demer L.L., Skinner H.C. and Koos B.J. (2001). Placental calcification: A metastatic process? Placenta 22, 591-596.

Portera-Cailliau C., Price D.L. and Martin L.J. (1997). Non-NMDA and NMDA receptor-mediated excitotoxic neuronal deaths in adult brain are morphologically distinct: further evidence for an apoptosis-necrosis continuum. J. Comp. Neurol. 378, 88-104.

Postler E., Lehr A., Schluesener H. and Meyermann R. (1997). Expression of the S-100 proteins MRP-8 and -14 in ischemic brain lesions. Glia 19, 27-34.

Rodriguez M.J., Ursu G., Bernal F., Cusi V. and Mahy N. (2001). Perinatal human hypoxia-ischemia vulnerability correlates with brain calcification. Neurobiol. Dis. 8, 59-68.

Saura J., Boatell M. L., Bendahan G. and Mahy N. (1995). Calcium deposit formation and glial reaction in rat brain after ibotenic acid-induced basal forebrain lesion. Eur. J. Neurosci. 7, 1569-1578.

Schwob J.E., Fuller T., Price J.L. and Olney J.W. (1980). Widespread patterns of neuronal damage following systemic or intracerebral injections of kainic acid: a histological study. Neuroscience 5, 991-1014.

Seitelberger F., Lassmann H. and Hornykiewicz O. (1990). Some mechanisms of brain edema studied in a kainic acid model. Acta Neurobiol. Exp. (Warsz) 50, 263-267.

Sperk G. (1994). Kainic acid seizures in the rat. Prog. Neurobiol. 42, 1-32.

Sperk G., Lassmann H., Baran H., Kish S.J., Seitelberger F. and Hornykiewicz O. (1983). Kainic acid induced seizures: neurochemical and histopathological changes. Neuroscience 10, 1301-1315.

Sperk G., Lassmann H., Baran H., Seitelberger F. and Hornykiewicz O. (1985). Kainic acid-induced seizures: dose-relationship of behavioural, neurochemical and histopathological changes. Brain Res. 338, 289-295.

Stewart G.R., Olney J.W., Schmidt R.E. and Wozniak D.F. (1995). Mineralization of the globus pallidus following excitotoxic lesions of the basal forebrain. Brain Res. 695, 81-87.

Streit W.J., Walter S.A. and Pennell N.A. (1999). Reactive microgliosis. Prog. Neurobiol. 57, 563-581.

Trump B.F., Berezesky I.K., Smith M.W. and Phelps P.C. (1992). The role of ionized cytosolic calcium ([$Ca2^{+}$]i) in injury and recovery from anoxia and ischemia. Md. Med. J. 41, 505-508.

Tuunanen J., Lukasiuk K., Halonen T. and Pitkanen A. (1999). Status epilepticus-induced neuronal damage in the rat amygdaloid complex: distribution, time-course and mechanisms. Neuroscience 94, 473-495.

Vakaet A., Rubens R., de Reuck J. and van der Eecken H. (1985). Intracranial bilateral symmetrical calcification on CT-scanning. A case report and a review of the literature. Clinic. Neurol. Neurosurg. 87, 103-111.

Vermersch P., Leys D., Pruvo J.P., Clarisse J. and Petit H. (1992). Parkinson's disease and basal ganglia calcifications: prevalence and clinico-radiological correlations. Clinic. Neurol. Neurosurg. 94, 213-217.

Whetsell W.O., Jr. (1996). Current concepts of excitotoxicity. J. Neuropathol. Exp. Neurol. 55, 1-13.

Wisniewski K.E., French J.H., Rosen J.F., Kozlowski P.B., Tenner M. and Wisniewski H.M. (1982). Basal ganglia calcification (BGC) in Down's syndrome (DS)--another manifestation of premature aging. Ann. NY Acad. Sci. 396, 179-189.

Accepted April 4, 2003